



## Removal of *p*-nitrophenol (PNP) in aqueous solution by the micron-scale iron–copper (Fe/Cu) bimetallic particles



Bo Lai <sup>a,\*</sup>, Yunhong Zhang <sup>a</sup>, Zhaoyun Chen <sup>a</sup>, Ping Yang <sup>a</sup>, Yuexi Zhou <sup>b</sup>, Juling Wang <sup>b</sup>

<sup>a</sup> Department of Environmental Science and Engineering, School of Architecture and Environment, Sichuan University, No. 24 South Section 1, Yihuan Road, Chengdu 610065, China

<sup>b</sup> Research Center of Water Pollution Control Technology, Chinese Research Academy of Environmental Sciences, Beijing 100012, China

### ARTICLE INFO

#### Article history:

Received 23 April 2013

Received in revised form 9 August 2013

Accepted 14 August 2013

Available online 21 August 2013

#### Keywords:

*p*-Nitrophenol (PNP)

Zero valent iron (ZVI)

Fe/Cu bimetallic particles

Degradation products

Wastewater treatment

### ABSTRACT

In this study, in order to further investigate the degradation capacity and mechanism of Fe/Cu bimetallic system, the prepared Fe/Cu bimetallic particles with different theoretical copper mass loadings (0.05, 0.11, 0.24, 0.41, 0.62, 0.89, 1.26 and 1.81 g Cu/g Fe) were characterized by SEM, EDS, XRD and laser particle size analyzer. Also, the effect of theoretical Cu mass loading and five key operating parameters on the PNP removal efficiency was investigated thoroughly. Furthermore, the mineralization process of PNP was studied by using COD, TOC, UV-vis spectra, FTIR spectra and GC/MS. The results show that a large number of fine Cu particles were produced from the excessive theoretical Cu mass loading, and they facilitated the catalytic reactivity of the Fe/Cu bimetallic particles at Cu loading <0.89 g Cu/g Fe. Additionally, the heterogeneous Cu layer is also favor for the catalytic reactivity of the Fe/Cu bimetallic particles, while the uniform and dense Cu layer can decrease its reactivity severely. The degradation rates of PNP by the Fe/Cu particles with different theoretical Cu mass loadings are all in accordance with the pseudo-first-order kinetics model, and the optimal operating parameters were obtained by the batch experiments. In addition, both the indirect reduction by atomic hydrogen and the direct reduction on the catalytic activity sites play a leading role on the pollutants removal. Finally, the degradation pathway of PNP was proposed according to the detected intermediates by GC/MS. Collectively, these results suggest that the Fe/Cu bimetallic system should be proposed as a cost-effective pretreatment process for the toxic and refractory PNP wastewater.

© 2013 Elsevier B.V. All rights reserved.

### 1. Introduction

Nowadays, industrial wastewater containing aromatic pollutants represent a big challenge for the researchers. *p*-Nitrophenol (PNP) and its derivatives all are the typical aromatic pollutants discharged from dyes, explosives, pesticides, plasticizers and herbicides industries [1]. All these compounds in industrial wastewater are toxic and refractory organic pollutants, and most of them are considered as hazardous wastes and priority toxic pollutants by the US Environmental Protection Agency (EPA). However, these pollutants are usually hard to be treated directly by the traditional biological treatment process due to their high toxicity and low biodegradability [2]. Advanced oxidation processes (AOPs) including Fenton reagent [3], electro-Fenton [4], photocatalysis [5,6], catalytic wet air oxidation [7] and microwave assisted oxidation process [8] were usually used to degrade these toxic and refractory

PNP. However, all of these AOPs suffer from the limitations of high costs.

Zero-valent iron (ZVI) and Fe/GAC micro-electrolysis have been used to treat the toxic and refractory wastewater including dye wastewater [9], atrazine [10], and ABS resin wastewater [11]. Despite the widespread studies on these treatment technologies, their practical applications are still suffering from many limitations. In particular, these systems will lose their reactivity over time resulted from the corrosion products or other precipitates on the surface of the Fe<sup>0</sup> and GAC [12]. One strategy that has proven effective in overcoming some shortcomings of ZVI and Fe/GAC micro-electrolysis involves the addition of Cu pieces into ZVI reactor. The Fe–Cu process is developed by the thorough mixture of iron scrap and Cu pieces in a desired proportion [13]. High reaction potential can improve reduction capacity of Fe<sup>0</sup>, and a higher pollutant removal efficiency would be obtained even in neutral pH range [14,15]. However, the mixture of Fe<sup>0</sup> and Cu<sup>0</sup> shavings are put to form a fixed bed in the Fe–Cu process, and the fixed bed structure can limit the mass transport rates of intermediates, products and reactants between the solution phase and the Fe<sup>0</sup>/Cu<sup>0</sup> surfaces.

\* Corresponding author. Tel.: +86 18682752302; fax: +86 18682752302.

E-mail address: [laibo1981@163.com](mailto:laibo1981@163.com) (B. Lai).

Recently, the micron-scale bimetallic reductants prepared by the deposition of a second transition metal on the iron surface can enhance rates of the pollutants reduction remarkably [16–20]. The previous studies suggest that the transition metal involving Ni, Pd, Cu, Co, Au and Ru can enhance the catalytic reactivity of Fe<sup>0</sup> [20–22]. Somehow, these transition metals have different reactivity enhancements for the prepared bimetallic reductants. Cwiertny et al. [22] found the following reactivity trend of the prepared bimetallic reductants towards 1,1,1-TAC: Ni/Fe ≈ Pd/Fe > Cu/Fe > Co/Fe > Au/Fe ≈ Fe. Lin et al. [20] also found that the catalytic activity of the noble metal followed the order of Pd > Ru > Pt > Au. Two types of catalytic mechanisms of the bimetallic reductants have been proposed by the previous researchers, (a) indirect reduction by the atomic hydrogen ([H]<sub>abs</sub>) absorbed on the surface of bimetallic reductants, and the transition metal additives can facilitate the generation of surface-bond atomic hydrogen ([H]<sub>abs</sub>) [20,21], (b) direct reduction on the catalytic activity site by accepting electrons from the oxidation of Fe<sup>0</sup>, and the surface additives (i.e., transition metal) can increase the oxidation of Fe<sup>0</sup> through the formation of infinite galvanic cells [13,14,23]. At present, the prepared bimetallic reductants were mainly used to reduce the lower concentration organohalides (such as 1,1,1-trichloroethane) [22]. The experiment results of Bransfield et al. [21] show that surface-bond atomic hydrogen ([H]<sub>abs</sub>) plays a leading role on the reduction of organohalide, while Xu et al. consider that the dechlorination is mainly resulted from the direct reduction on the surface of catalytic activity site (Cu) [13].

The previous studies mainly show that Fe/Cu bimetallic reductant with low Cu loading (<10 μmol Cu/g Fe) was used to reduce the organohalide with low initial concentration (<100 μmol/L) [21,24]. Also, their results reveal a more modest rate of increase in the  $K_{obs}$  at Cu loading <10 μmol Cu/g Fe [24]. However, the Fe/Cu bimetallic reductant has not been used to treat the higher concentration organic pollutants, and the effect of Cu loading on the degradation of higher concentration organic pollutants might be completely different.

Therefore, it is important to further investigate the operating parameters and catalytic mechanism of the prepared Fe/Cu bimetallic system for the treatment of higher concentration pollutants. In the present investigation, we have setup experiments specifically to study the effect of theoretical copper mass loadings and operating parameters on the pollutant removal efficiency by Fe/Cu bimetallic system. The prepared Fe/Cu bimetallic particles with different theoretical copper mass loadings were characterized by scanning electron microscopy (SEM), energy dispersive X-ray spectroscopy (EDS), X-ray diffraction (XRD) and laser particle size analyzer. Furthermore, effect of theoretical Cu mass loading, Fe/Cu bimetallic dosage, initial PNP concentration, initial pH, electrolyte and stirring speed on the PNP removal efficiency was

investigated, respectively. Additionally, the mineralization of PNP was studied by analyzing the variation of COD, TOC, UV-vis and FTIR spectra after treatment of Fe/Cu bimetallic system. Finally, the degradation products of PNP by the Fe/Cu bimetallic system were analyzed using a gas chromatography-mass spectrometry (GC/MS), and the degradation pathway was proposed according to the detected intermediates.

## 2. Experimental

### 2.1. Reagents

PNP (99%), CuSO<sub>4</sub>·5H<sub>2</sub>O (analytical reagent), Na<sub>2</sub>SO<sub>4</sub> (analytical reagent) and zero valent iron (ZVI) powders from Chengdu Kelong chemical reagent factory were used in the experiment. The zero valent iron powders have mean particle size of approximately 120 μm, and their iron content reaches approximately 97%. Dichloromethane (HPLC grade) were obtained from J.T. Baker (Deventer, The Netherlands). Other chemicals used in the experiment were of analytical grade. Deionized water was used throughout the whole experiment process.

### 2.2. Preparation of the iron–copper (Fe/Cu) bimetallic particles

The micron-scale zero valent iron powder was used as the base material for the preparation of iron–copper (Fe/Cu) bimetallic particles. Prior to plating, iron particles were not needed acid washing by HCl, since there was no iron oxide to be detected on the surface of iron particles by SEM–EDS (Fig. 1(a))

). The iron–copper (Fe/Cu) bimetallic particles were prepared by the displacement plating, via adding 200 mL of CuSO<sub>4</sub> solution to the iron particles. After the CuSO<sub>4</sub> solution was added to the iron particles, the slurry was mixed by hand for 10 min. Then the prepared Fe/Cu bimetallic particles were separated from the supernatant after 5 min precipitation process. Finally, the separated Fe/Cu bimetallic particles were rinsed three times with deionized water, once with ethanol, and then were dried under N<sub>2</sub> protection at 80 °C for 40 min.

CuSO<sub>4</sub> was used to deposit Cu on the surface of iron particles by the iron–copper replacement reaction, and the Cu mass loading on the surface of iron particles (i.e., Fe/Cu ratio) could affect the catalytic activity of the prepared Fe/Cu bimetallic particles [21,22]. In addition, the copper mass loading of the prepared Fe/Cu bimetallic particles could be changed by adjusting the concentration of CuSO<sub>4</sub> solution. In order to prepare the Fe/Cu bimetallic particles with different theoretical copper mass loadings, 15 g iron particles were added in 200 mL CuSO<sub>4</sub> solution with different concentration (specifically, 9.38, 18.75, 37.50, 56.25, 75.00, 93.75, 112.50 and 131.25 g/L), respectively. Immersion plating with these solution

**Table 1**  
The parameter of the prepared Fe/Cu bimetallic particles with different Fe/Cu ratio.

Fe/Cu <sup>a</sup>	M <sub>Fe</sub> (g)	M <sub>Cu</sub> (g)	C <sub>CuSO<sub>4</sub></sub> (g/L)	V <sub>CuSO<sub>4</sub></sub> (mL)	R <sub>Fe</sub>	TML <sub>Cu</sub> (g Cu/g Fe)	Fe/Cu <sup>b</sup>
20:1	15.00	0.75	9.38	200.00	14.34	0.05	10:0.5
10:1	15.00	1.50	18.75	200.00	13.69	0.11	10:1.1
10:2	15.00	3.00	37.50	200.00	12.38	0.24	10:2.4
10:3	15.00	4.50	56.25	200.00	11.06	0.41	10:4.1
10:4	15.00	6.00	75.00	200.00	9.75	0.62	10:6.2
10:5	15.00	7.50	93.75	200.00	8.44	0.89	10:8.9
10:6	15.00	9.00	112.50	200.00	7.13	1.26	10:12.6
10:7	15.00	10.50	131.25	200.00	5.81	1.81	10:18.1

<sup>a</sup> Mass ratio of zero iron particles with Cu in CuSO<sub>4</sub> solution before replacement reaction.

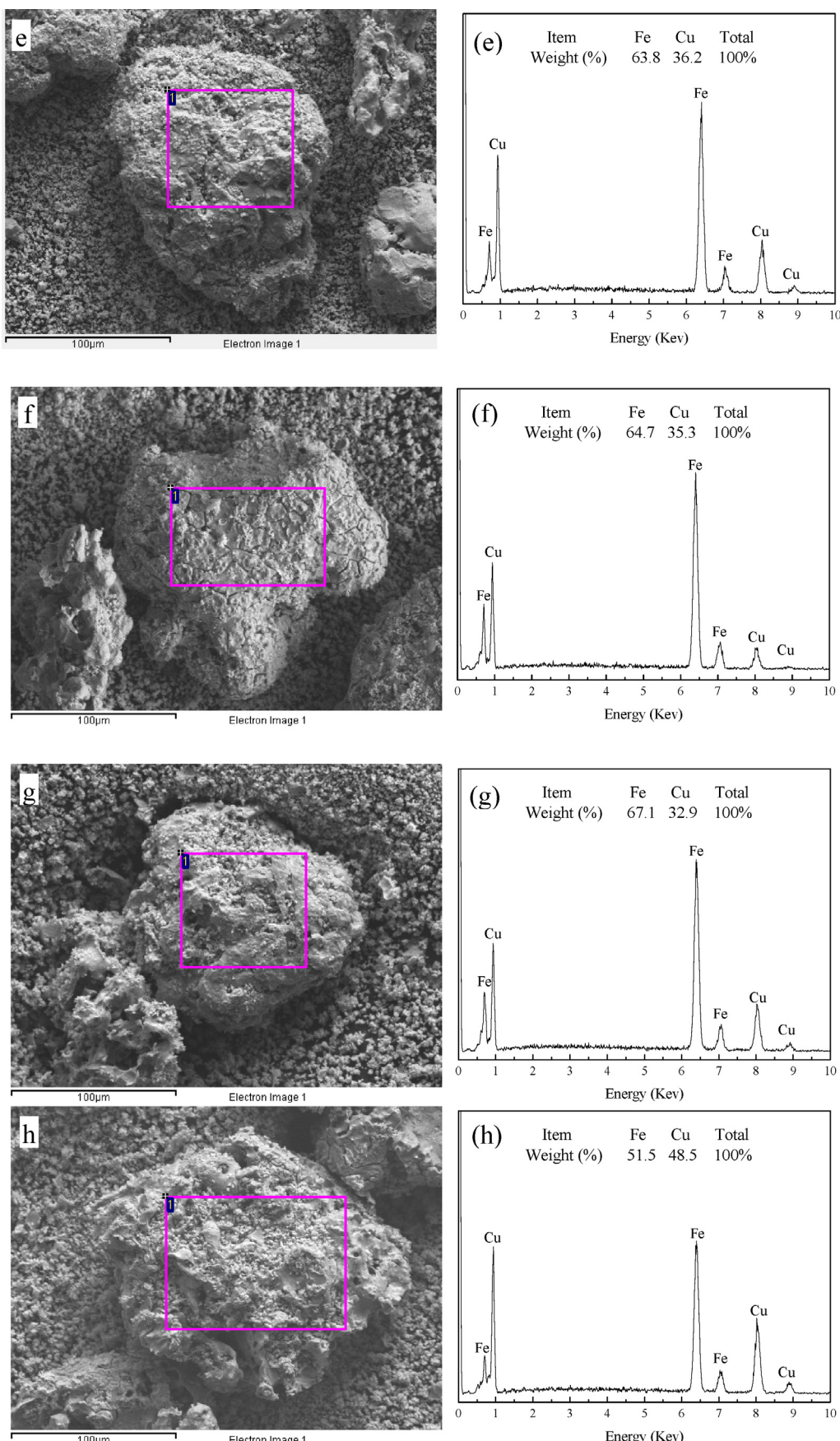
<sup>b</sup> Mass ratio of Fe with Cu in the prepared Fe/Cu bimetallic particles after replacement reaction.

M<sub>Fe</sub>: The mass of zero iron particles which added in the CuSO<sub>4</sub> solution.

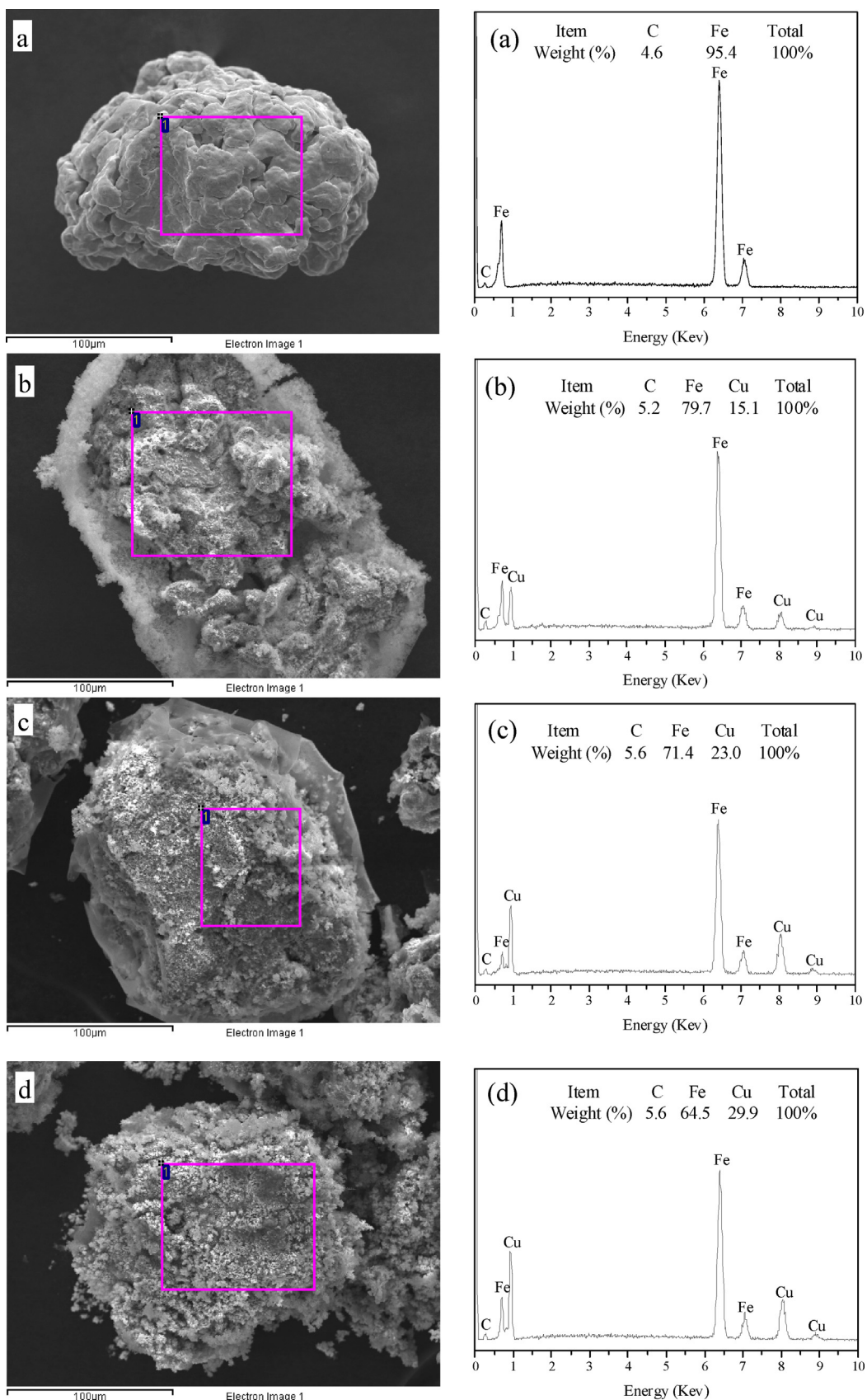
: The mass concentration of CuSO<sub>4</sub> solution.

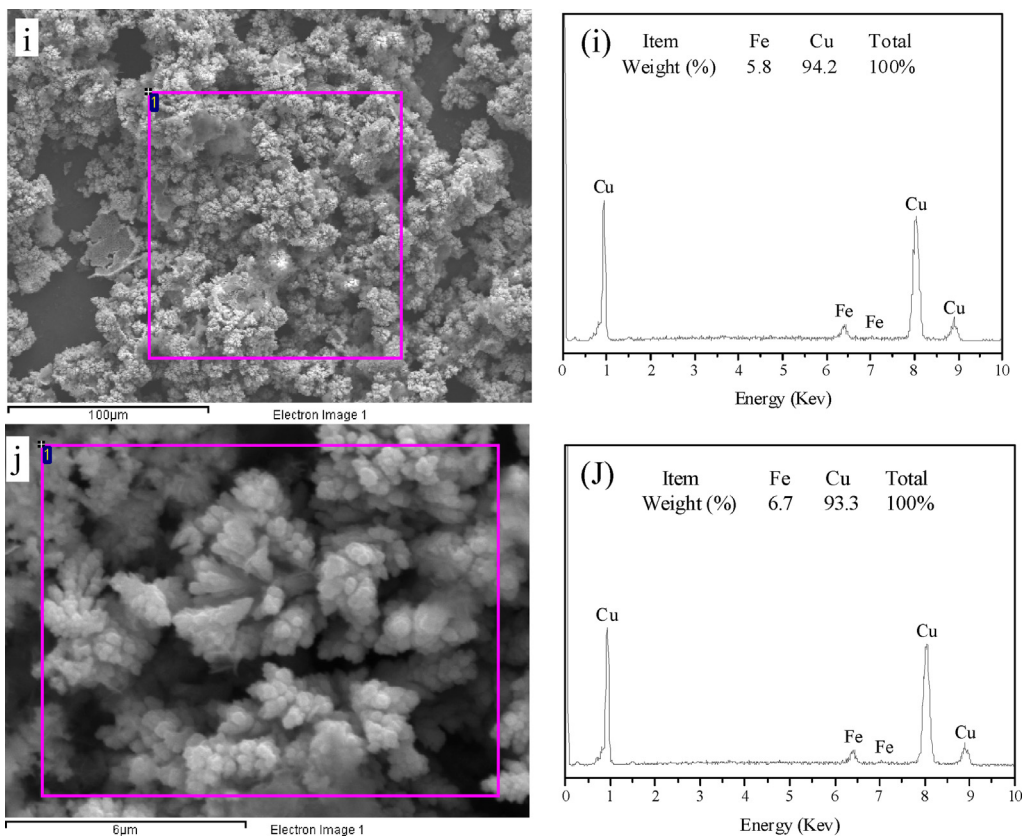
R<sub>Fe</sub>: The mass of Fe in the prepared Fe/Cu bimetallic particles after replacement reaction.

TML<sub>Cu</sub>: Theoretical Cu mass loading on the surface of iron particles.



**Fig. 1.** SEM and EDS spectra of zero valent iron ( $\text{Fe}^0$ ) particles and iron–copper ( $\text{Fe}/\text{Cu}$ ) bimetallic particles with different theoretical Cu mass loadings: (a) zero valent iron ( $\text{Fe}^0$ ) particles; (b) 0.11 g Cu/g Fe; (c) 0.24 g Cu/g Fe; (d) 0.41 g Cu/g Fe; (e) 0.62 g Cu/g Fe; (f) 0.89 g Cu/g Fe; (g) 1.26 g Cu/g Fe; (h) 1.81 g Cu/g Fe; ((i), (j)) shedding copper particles with small particle size.

**Fig. 1.** (Continued)

**Fig. 1.** (Continued).

resulted in theoretical Cu mass loadings of 0.05, 0.11, 0.24, 0.41, 0.62, 0.89, 1.26 and 1.81 g Cu/g Fe, calculated by the iron–copper replacement reaction equation (Table 1). After 15 min iron–copper replacement reaction, there were no copper ions detected in the reaction solution by atomic absorption spectroscopy (AA-6300, Shimadzu, Japan), which suggests that the copper ions should be replaced by iron completely. Therefore, the value of theoretical Cu mass loading calculated by the iron–copper replacement reaction equation was valid. Also, the parameters of the prepared Fe/Cu bimetallic particle with different ratios are shown in Table 1.

### 2.3. Apparatus and experimental procedure

The reactivity of the prepared Fe/Cu bimetallic particles was investigated by batch experiments. The *p*-nitrophenol (PNP) was used as a model pollutant in this study, and the PNP stock solution (100–1000 mg/L) was prepared with Na<sub>2</sub>SO<sub>4</sub> (0–50 mmol/L) used as an electrolyte. Also, the PNP aqueous solution was not buffered, and its initial pH (3.0–9.0) was adjusted by adding diluted sulfuric acid (10%) or sodium hydroxide solutions (5 mol/L). In each batch experiment, 200 mL PNP aqueous solution (100–1000 mg/L) and the desired dosage of Fe/Cu bimetallic particles (5–45 g/L) were added in a 500 mL flat bottom beaker, and the slurry was mixed by a mechanical stirrer (0–400 r/min). And the whole experiment was performed at 25 ± 2 °C by water bath heating.

In this study, the key effect factors, such as theoretical Cu mass loading (0–1.81 gCu/gFe), Fe/Cu bimetallic particles dosage (5–45 g/L), initial PNP concentration (100–1000 mg/L), initial pH (3.0–9.0), electrolyte (Na<sub>2</sub>SO<sub>4</sub>) concentration (0–50 mmol/L) and stirring speed (0–400 r/min), were investigated thoroughly by the batch experiments. Samples were taken from the reactive beaker at regular intervals (5 min) by withdrawing 1 mL of

sample solution. And then the residual PNP concentration, COD and TOC of the effluent were measured by reversed-phase HPLC chromatography (Agilent, USA), COD analyzer (Lianhua, China) and TOC analyzer (Shimazu, Japan), respectively. In order to compare the catalytic reactivity of Fe/Cu bimetallic particles with zero valent iron particles (ZVI), under the same operating conditions (initial pH = 6.7, [PNP]<sub>0</sub> = 500 mg/L, [Na<sub>2</sub>SO<sub>4</sub>]<sub>0</sub> = 50 mmol/L, [Fe/Cu]<sub>0</sub> = 35 g/L, [Fe<sup>0</sup>]<sub>0</sub> = 35 g/L, the theoretical Cu mass loading was 0.89 g Cu/g Fe, stirring speed was 400 r/min), the treatment effluent of the two batch experiments both were analyzed by COD analyzer (Lianhua, China), TOC analyzer (Shimazu, Japan), UV-vis spectrophotometer (Shimazu, Japan) and Fourier transform infrared spectroscopy (FTIR, Perkin Elmer 100, USA). Additionally, the total iron in the effluent of the two batch experiments was measured by using atomic absorption spectrometry (AA-6300, Shimadzu, Japan). Finally, the degradation pathway of PNP by the prepared Fe/Cu bimetallic particles were investigated according to the degradation products of PNP detected by gas chromatography mass spectrometry (GC/MS) with standard samples.

### 2.4. Analytical methods

#### 2.4.1. Scanning electron microscopy (SEM) and energy dispersive spectrometer (EDS)

The surface morphologies of the prepared Fe/Cu bimetallic particles were observed by S-3500N scanning electron microscopy (SEM, Hitachi, Japan). In addition, the surface elementary composition of Fe/Cu bimetallic particles was analyzed by energy dispersive spectrometry (EDS). And EDS analysis was carried out by a permanent thin film window link (Oxford Instruments) detector and WinEDS software in a Hitachi S-3500N scanning electron

microscope (SEM). At the end, this instrument was operated at 25 kV and emission current of 60–70  $\mu\text{A}$ .

#### 2.4.2. X-ray diffraction

On the basis of the elemental composition analysis for the prepared Fe/Cu bimetallic particles by EDS, its compound composition was further investigated by X-ray diffraction (XRD) analysis. The XRD analysis was performed by a Phillips Xpert Pro diffractometer with a Cu  $K_{\alpha}$  radiation source ( $\lambda = 1.5406 \text{ \AA}$ ) operating at 40 keV and a tube current of 30 mA. XRD spectra were acquired between  $2\theta$  of 10–100, with a step size of 0.05 and a 2 s dwell time [12].

#### 2.4.3. FTIR and UV-vis adsorption spectrum

Fourier transform infrared spectroscopy (FTIR) was used to assess the differences in the general functional groups of the influent and effluent of the zero valent iron (ZVI) control experiment and Fe/Cu bimetallic particles. 300 mg KBr was milled and compressed into a pellet with force of 10 t applied for 1 min. The pellet was then scanned using a Perkin Elmer 100 FTIR spectrometer and the background spectra were generated using its software. To obtain the spectra for the influent and effluent of the two batch experiments, the samples were first dried and grinded, and then each sample (6 mg) was mixed with 300 mg KBr and milled into powder [25]. The powder mixture was compressed into a pellet under 10 t force for 1 min. Each sample was scanned four times between the wavelengths of 4000 and 400  $\text{cm}^{-1}$ .

The UV-vis absorption spectra of the influent and effluent of the two batch experiments were carried out in 10 mm quartz cuvettes, and the UV-vis spectra were recorded from 190 to 550 nm using deionized water as blank.

#### 2.4.4. Gas chromatography-mass spectrometry (GC/MS)

In our previous work, a gas chromatography-mass spectrometry (GC/MS) analytic method was setup to qualitatively determine the degradation products of PNP [1]. Prior to GC/MS determination, a 50 mL sample was extracted using 10 mL dichloromethane three times under acidic ( $\text{pH} \approx 2.0$ ), neutral ( $\text{pH} \approx 7.0$ ) and alkaline ( $\text{pH} \approx 12.0$ ) conditions, respectively. The three extracted layers were mixed, dehydrated and dried under nitrogen atmosphere. The residue was dissolved in 1.0 mL  $\text{CH}_2\text{Cl}_2$  and 1 mL was injected into a 7890/5975 GC/MS system (Agilent, USA) equipped with a HP-5MS capillary column. The GC column was operated in temperature programmed mode at 40 °C for 3 min, raised at  $10 \text{ }^{\circ}\text{C min}^{-1}$  to 280 °C, and held for 5 min. The solvent delay was 6 min and the total run time was 32 min. The mass range scanned was 20–500 m/z. The qualitative analysis of degradation products was carried out with reference to the NIST05 mass spectral library database. And the detected degradation products would be further confirmed by the standard samples.

#### 2.4.5. Other analysis methods

The concentration of PNP in the samples was achieved by reversed-phase HPLC chromatography (Agilent USA) equipped with the Eclipse XDB C-18 (5  $\mu\text{m}$ , 250 × 4.6 mm). The binary phase were (A) water with 0.1%  $\text{H}_3\text{PO}_4$  and (B) acetonitrile, and the eluent was A and B (1:1, v/v) with a flow rate of 0.8 mL/min. Detection was performed using a G1365MWD UV detector set at 317 nm for PNP. The particle size distribution of the prepared Fe/Cu bimetallic particles was determined by Mastersizer 2000 laser particle size analyzer (Malvern, England). Total iron of the effluent was determined by atomic absorption spectrometry (AA-6300, Shimadzu, Japan). The COD and TOC of the influent and effluent were analyzed by COD analyzer (Lianhua, China) and TOC analyzer (Shimazu, Japan), respectively.

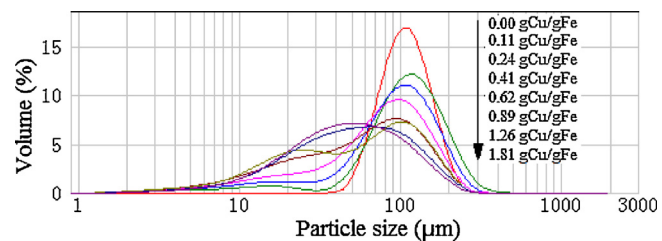


**Fig. 2.** Particle size distribution of Fe/Cu bimetallic particles with different theoretical Cu mass loadings.

## 3. Results and discussion

### 3.1. Characterization of Fe/Cu bimetallic particles

The surface morphology, elementary composition, compound structure and particle size distribution of the prepared Fe/Cu bimetallic particles were observed and evaluated by SEM, EDS, XRD and laser particle size analyzer, respectively. Since the catalytic activity of the prepared Fe/Cu bimetallic particles could be affected by the Cu mass loading [21,22], the characterization of bimetallic particles with different Cu mass loading (specially, 0, 0.11, 0.24, 0.41, 0.62, 0.89, 1.26 and 1.81 g Cu/g Fe) were analyzed by the above-mentioned methods.

**Fig. 1(a)** shows the SEM image and EDS spectrum of ZVI without Cu loading, while **Fig. 1(b)–(h)** show the SEM images and EDS spectra of the prepared Fe/Cu bimetallic particles with different theoretical Cu mass loadings (i.e., 0.11, 0.24, 0.41, 0.62, 0.89, 1.26 and 1.81 g Cu/g Fe). As shown in **Table 1**, the theoretical Cu mass loading was calculated according to the iron particles dosage and  $\text{CuSO}_4$  concentration in the prepared process of Fe/Cu bimetallic particles. It could be seen from **Fig. 1(a)** that the morphology of ZVI particle was sponginess and smoothing, and only two elements of C (4.6 wt%) and Fe (95.4 wt%) were detected by EDS on the surface of the ZVI particles. Therefore, the ZVI particles could not be acid washed to remove oxide compounds, although these particles were usually to be acid washed by HCl before replacement process in other similar experiments [18,21,26].

It could be seen from the SEM images and EDS spectra in **Fig. 1(b)–(h)** that both of the two elements of Fe and Cu were detected on the surface of the prepared Fe/Cu bimetallic particles. Furthermore, the weight ratio of Fe decreased from 79.7% to 51.5% with theoretical Cu mass loading increasing from 0.11 to 1.81 g Cu/g Fe, while the weight ratio of Cu increased from 15.1% to 48.5%. Meanwhile, weight ratios of Fe and Cu changed quickly when theoretical Cu mass loading increased from 0.11 to 0.62 g Cu/g Fe, and then their changes were tending towards stability. Moreover, it can be observed from SEM images in **Fig. 1(d)–(h)** that a large number of fine particles were formed when theoretical Cu mass loading was higher than 0.41 g Cu/g Fe. And **Fig. 1(i)–(j)** shows that the formed fine Cu particles were wheat-ear-like and their main elemental constituent was Cu (approximately 90 wt%). The results suggest that the planting Cu could not deposit completely on the surface of iron particles when theoretical Cu mass loading reached 0.41 g Cu/g Fe, and the excessive Cu would drop off from the surface of iron particles to form a large number of fine Cu particles. Bransfield and Cwiertny also found that 100% plating efficiency would not be obtained for Cu plating solutions that contained >70  $\mu\text{mol Cu/g Fe}$  [24]. Therefore, Fe and Cu ratios were tending towards stability when the theoretical Cu mass loading was higher than 0.41 g Cu/g Fe. **Fig. 2** shows particle size distribution of the Fe/Cu bimetallic particles with different theoretical Cu mass loadings. It is clear that the volume ratio of the particles with a size distribution of 40–300  $\mu\text{m}$  was decreasing from 100% to 50% with

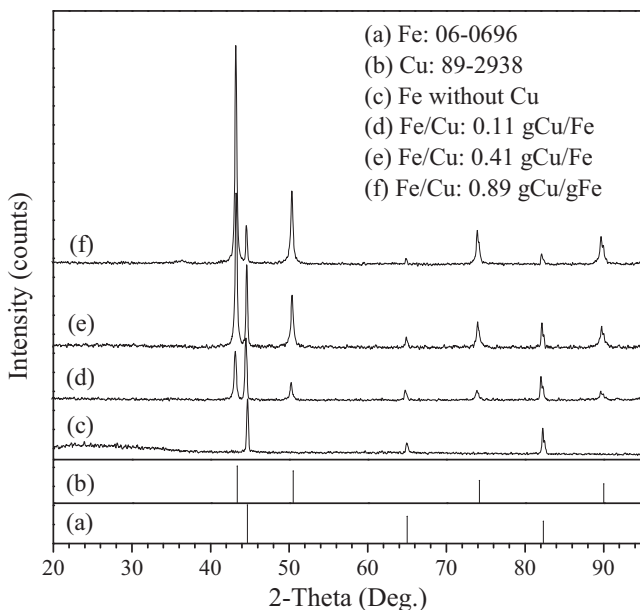


**Fig. 3.** XRD patterns of zero valent iron ( $\text{Fe}^0$ ) particles and iron–copper (Fe/Cu) bimetallic particles with different Fe/Cu ratios.

theoretical Cu mass loading increasing, while that of the particles with a size distribution of 1–40  $\mu\text{m}$  was increasing from 0% to 50% gradually. What's more, the volume ratio of the particles (1–40  $\mu\text{m}$ ) increased quickly when the theoretical Cu mass loading was higher than 0.41 g Cu/g Fe. The results also proved that the fine Cu particles were produced from the excessive theoretical Cu mass loading.

### 3.2. XRD analysis of Fe/Cu bimetallic particles

In order to further confirm that there was not any by-product (such as the oxide compound of Fe or Cu) generated in the prepared process of Fe/Cu bimetallic particles, the iron and bimetallic particles were further analyzed by XRD on the basis of SEM-EDS analysis. The representative XRD spectra for these particles with different theoretical Cu mass loadings are shown in Fig. 3. The XRD pattern in Fig. 3 indicates that the chemical composition of the prepared Fe/Cu bimetallic particles were predominantly iron and copper. There was not any oxide compound to be detected by XRD. Also, the diffraction peaks ( $2\theta=43.3^\circ$ ,  $50.4^\circ$ ,  $74.1^\circ$ ,  $89.9^\circ$ ) corresponding to Cu increase quickly with the increasing theoretical Cu mass loading, which indicates that the Cu was deposit on the surface of iron successfully by replacement reaction. The results suggest that there was almost no by-product in the prepared process even under the unsealed and non-nitrogen protection conditions. This phenomenon can be explained from two aspects, (a) since the replacement reaction was performed in the aqueous solution was under a lower mixing speed, oxygen in air were hard to dissolve in aqueous solution; (b) the amount of oxygen in aqueous solution was very low, so the producing oxide compounds could be ignored completely. Therefore, the Fe/Cu bimetallic particles can be produced under the air circumstance, which can save costs from closeness and nitrogen protection. And this prepared method are different from other previous studies [21,24].

### 3.3. Effect of the Cu layer structure characteristics on the pollutant removal

It could be seen from Fig. 1(b)–(h) that the Cu additive layer was a heterogeneous and loose film on the surface of Fe/Cu bimetallic particles. These results are similar to other studies of

bimetallic particles [21,24]. The loose and heterogeneous surface structure characteristics may be in favor of catalytic efficiency of the Fe/Cu bimetallic particles. In order to prove this hypothesis, a control experiment was setup. In the control experiment, the Fe/Cu bimetallic particles with a uniform and dense Cu layer were prepared by adding edetate disodium (EDTA-2Na) in the  $\text{CuSO}_4$  solution. EDTA-2Na as a stabilizer can form stable complexes with Fe and Cu, which is in favor of refining the grain and forming an uniform and dense copper planting layer on the surface of bimetallic particles [22,27,28]. Fig. 4 shows that these Fe/Cu bimetallic particles had a uniform and dense surface morphology, and the weight ratio of Cu element reached approximately 90% on the surface of bimetallic particle. In other words, these Fe/Cu bimetallic particles were covered by a uniform and dense Cu layer. However, under the same theoretical Cu mass loading and other operating conditions, the pollutant treatment efficiency of these Fe/Cu bimetallic particles was much lower than that of the Fe/Cu bimetallic particles prepared without EDTA-2Na, and their treatment efficiency was even lower than that of ZVI particles without planting Cu layer. This phenomenon can be explained from two aspects, (a) the uniform and dense Cu layer can protect the internal iron and inhibit the corrosion reaction of iron, which also depress the catalytic reactivity of the Fe/Cu bimetallic particles; (b) the heterogeneous Cu layer is favor for the formation of Fe/Cu galvanic corrosion, which can enhance the catalytic reactivity of the Fe/Cu bimetallic particles.

### 3.4. Reaction kinetics of the prepared Fe/Cu bimetallic particles

In order to measure the reaction kinetics of the prepared Fe/Cu bimetallic particles towards organic pollutants, the batch experiments with the bimetallic particles were setup to treat PNP aqueous solution. In the batch experimental process, the key effect factors, such as theoretical Cu mass loading, Fe/Cu bimetallic dosage, initial PNP concentration, initial pH, electrolyte concentration ( $\text{Na}_2\text{SO}_4$ ) and stirring speed, on the removal efficiency of PNP were investigated thoroughly. Meanwhile, the linear regression analysis of two-stage reaction described in details in references [1,29] was used to investigate the reaction kinetics of the prepared Fe/Cu bimetallic particles. The results of the degradation efficiency of PNP by Fe/Cu bimetallic particles under the different conditions are shown in Figs. 5 and 10.

#### 3.4.1. Effect of theoretical Cu mass loading on the catalytic reactivity

The previous authors found that the pollutant reduction in bimetallic system might occurs primarily at the surface of the transition metal additive (such as Cu on the surface of Fe) [21,22,24], and the Cu mass loading on the surface of Fe particles was a key influencing factor of the catalytic reactivity of the prepared Fe/Cu bimetallic particles [24]. Thus, in order to further confirm the effect of theoretical Cu mass loading on the catalytic reactivity of the prepared Fe/Cu bimetallic particles, the batch experiments using the Fe/Cu bimetallic particles with different theoretical Cu mass loadings were performed in this study. Batch experiments were undertaken by adding 3.0 g Fe/Cu bimetallic particles into a flat bottom beaker ( $[\text{Fe}/\text{Cu}]_0 = 15 \text{ g/L}$ ), in which each beaker including 200 mL of PNP stock solution with an initial PNP concentration of 500 mg/L, initial pH at 6.7 and  $\text{Na}_2\text{SO}_4$  concentration of 50 mmol/L. Then the reaction was processed in the present of mechanical stirring (400 r/min) at operating temperature  $25 \pm 2^\circ\text{C}$ . At the end, PNP residual concentration was determined after the treatment by the Fe/Cu bimetallic system.

The logarithmic plots of residual concentration of PNP in solutions versus the reaction time are shown in Fig. 5(a), which illustrates that a good linear fitting was observed in each of the batch experiments. The results indicate that the rates of

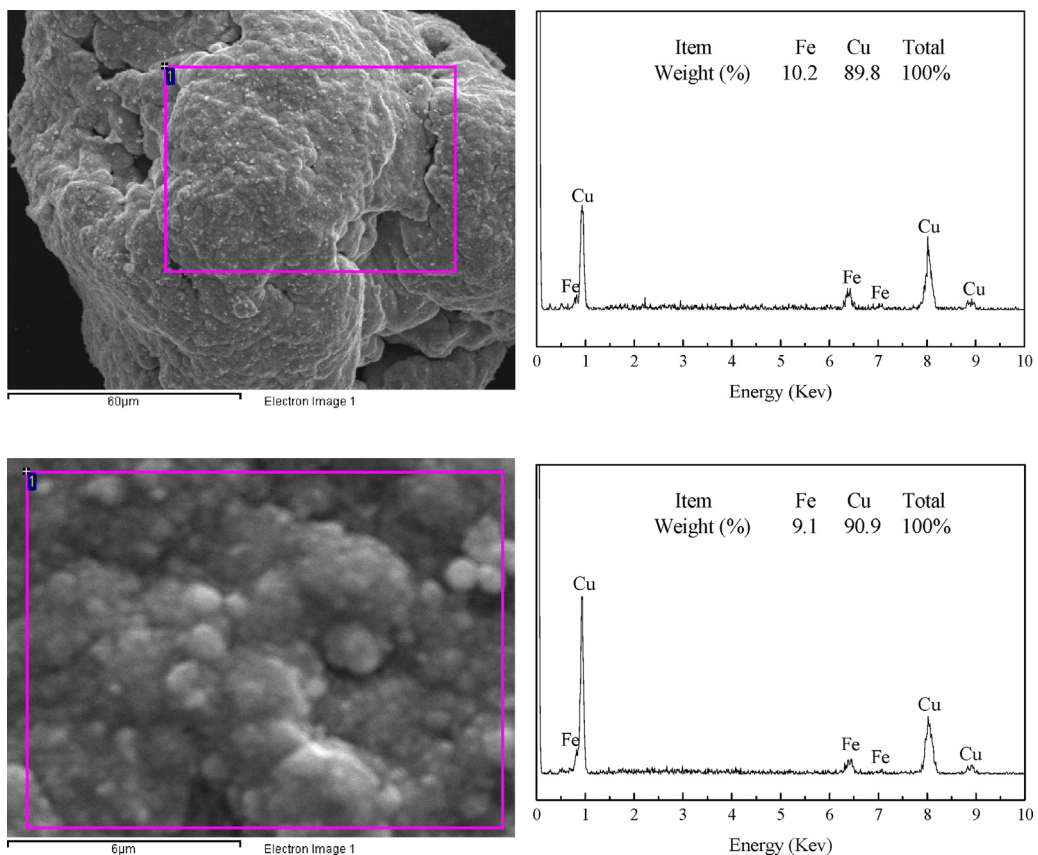


**Fig. 4.** SEM and EDS spectra of Fe/Cu bimetallic particles were prepared by adding EDTA-2Na in  $\text{CuSO}_4$  solution. (Theoretical Cu mass loading: 0.24 g Cu/g Fe).

PNP degradation by using the prepared Fe/Cu bimetallic particles with different theoretical Cu mass loadings all were described by the pseudo-first-order as shown in Eq. (1). A two-stage reaction occurred in the PNP degradation process by the prepared Fe/Cu bimetallic particles (Fig. 5). The initial stage (0–10 min), called rapid consumption of absorbed hydrogen ( $[\text{H}]_{\text{abs}}$ ) and occupation of the catalytic activity sites (Cu) on the surface of the Fe/Cu bimetallic particles, was explained by the proposed reaction mechanism of Fe/Cu bimetallic particles by the previous authors [13,21,30]. In this stage (0–10 min), PNP was degraded by two pathways, (a) indirect reduction of  $[\text{H}]_{\text{abs}}$ , (b) direct reduction on the catalytic activity sites (Cu) by the accepting electrons from the oxidation of  $\text{Fe}^0$ . According to the results, the initial stage reaction followed pseudo-first-order kinetics. The second stage was a slow reduction process where

residual PNP continued to be degraded by the newly generated  $[\text{H}]_{\text{abs}}$  and electrons transformed from iron. However, the second-stage reaction rate was limited seriously by the mass transport rates of intermediates, products and reactants between the solution phase and the Fe/Cu surfaces. And the similar results were occurred in the treatment process by zero valent iron (ZVI) [1,31]. The reaction in the second stage also followed pseudo-first-order kinetics. Additionally, the pseudo-first-order kinetic parameters are listed in Table S1 (supporting information). Thus the reaction rate in the initial stage was much higher than that in the second stage.

$$\ln \frac{[\text{PNP}]}{[\text{PNP}]_0} = -K_{\text{obs}} t \quad (1)$$

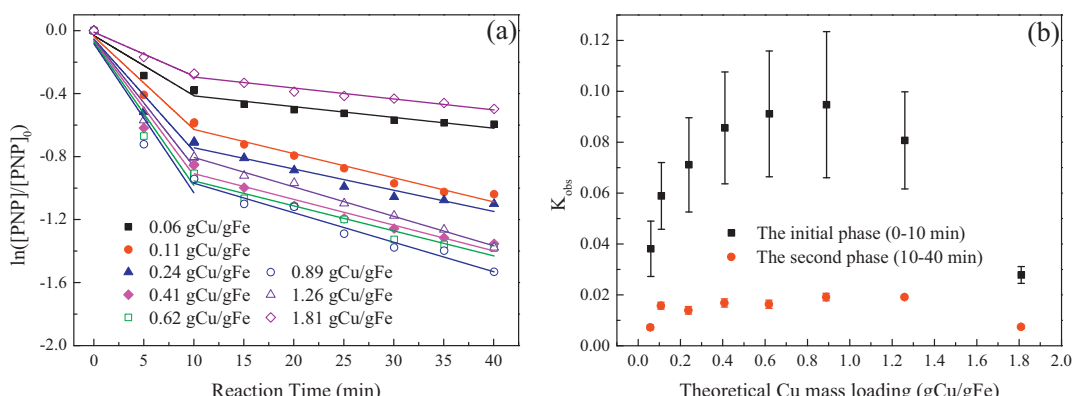


**Fig. 5.** Degradation kinetics for PNP by the prepared Fe/Cu bimetallic particles with different theoretical Cu mass loadings. Experiment conditions were:  $[\text{PNP}]_0 = 500 \text{ mg/L}$ , initial pH = 6.7,  $[\text{Na}_2\text{SO}_4]_0 = 50 \text{ mmol/L}$ ,  $[\text{Fe}/\text{Cu}]_0 = 15 \text{ g/L}$ , Stirring speed was 400 r/min.

Although the degradation rates of PNP by the Fe/Cu particles with different theoretical Cu mass loadings are all in accordance with the pseudo-first-order kinetics model, they have different  $K_{obs}$  which can be obtained by calculating the slope of the linear regression slope from Fig. 5(a). According to Fig. 5(b), it is clear that  $K_{obs}$  increases from 0.0381 to 0.0947 min<sup>-1</sup> with the increasing theoretical Cu mass loading from 0.06 to 0.89 g Cu/g Fe, and then it begins to decrease with the further increase of theoretical Cu mass loading at the initial phase (0–10 min). Meanwhile, the variation of  $K_{obs}$  at the second phase (10–40 min) is similar to that at the initial phase (0–10 min), but  $K_{obs}$  at the second phase (10–40 min) are much lower than that at the initial phase (0–10 min). The results suggest that the PNP degradation rate increase obviously with the increasing theoretical Cu mass loading, and it reached its maximum value when the Fe/Cu bimetallic particles holding a theoretical Cu mass loading of 0.89 g Cu/g Fe. This phenomenon can be explained from two aspects, (a) when theoretical Cu mass loading is lower than 0.89 g Cu/g Fe, the increase of theoretical Cu mass loading can enhance the contact area between Cu and Fe, which will improve the  $[H]_{abs}$  production, electron transport, catalytic sites and galvanic couple formation, (b) when theoretical Cu mass loading is higher than 0.89 g Cu/g Fe, the contact area between Cu and Fe will be decreased gradually because the ratio of Fe begins to lower than that of Cu, which goes against the  $[H]_{abs}$  production, electron transport, catalytic sites and galvanic couple formation. These results are similar to the effect of Fe/GAC ratios on the wastewater treatment efficiency by Fe/GAC system in our previous works [11,32].

The previous authors found that  $K_{obs}$  of the 1,1,1-trichloroethane (13.3 mg/L) degradation would not increase obviously when the Cu mass loading was higher than 10 μmol Cu/g Fe (i.e.,  $0.64 \times 10^{-3}$  g Cu/g Fe) [24]. However, Fig. 5(b) shows a high rate of increase in  $K_{obs}$  at theoretical Cu mass loadings <0.89 g Cu/g Fe in our study. The different results can be explained from three aspects, (a) PNP concentration (500 mg/L) in this study was much higher than that of 1,1,1-trichloroethane (13.3 mg/L) in previous experiment, and the pollutants concentration usually affect the degradation rate of the catalysts because the intermediates on the surface of catalysts will occupy catalytic sites or compete with the original pollutants for the catalytic sites [33,34]. Thus the catalytic sites of Fe/Cu particles cannot be occupied completely under the condition of the lower initial pollutant concentration, and it cannot response to the practical capacity of the Fe/Cu particles. (b) A large number of fine Cu particles (Fig. 1) formed from the excessive theoretical Cu mass loading will contact with the Fe surface of Fe/Cu particles under the condition of mechanical stirring, and this contact will increase catalytic site and galvanic couple, obviously. (c) Chemical property

of PNP and 1,1,1-trichloroethane are different, and the latter might be much more difficult to be reduced than the former, which resulted in the different  $K_{obs}$ . Under the optimal theoretical Cu mass loading of 0.89 g Cu/g Fe, the PNP removal efficiency only reached approximately 80%. The results reveal that Fe/Cu dosage (15 g/L) might not be enough for the complete degradation of PNP, and the optimization of Fe/Cu dosage will be performed in the following experiments.

### 3.4.2. Effect of Fe/Cu bimetallic dosage on the catalytic reactivity

Since dosage of catalysts can affect the degradation efficiency of the pollutants [1,35], batch experiments were setup and performed on a condition that different initial dosage of Fe/Cu bimetallic particles (5–45 g/L) were used to treat 500 mg/L of PNP aqueous solutions with the optimal theoretical Cu mass loading of 0.89 g Cu/g Fe. Mixed solutions were performed by mechanical stirring (400 r/min) at temperature 25 ± 2 °C. Fig. 6(a) shows the PNP degradation at different dosages of Fe/Cu bimetallic particles, which demonstrates that all followed the pseudo-first-order kinetics model and the pseudo-first-order kinetic parameters are listed in Table S2 (supporting information). Fig. 6(b) shows that the data were plotted as the  $K_{obs}$  against the Fe/Cu dosage. At the initial stage (0–10 min), the  $K_{obs}$  and Fe/Cu dosage have a good linear relationship and the correlation of determination ( $R^2$ ) reaches 0.93, which suggests that the  $K_{obs}$  is proportional to the Fe/Cu dosage and  $K_{obs}$  can be enhanced by elevating the Fe/Cu dosage. This phenomenon can be explained by the increased surface area,  $[H]_{abs}$ , catalytic site and galvanic couple formation when the Fe/Cu dosage increased. It is similar to the results observed by the previous authors [35], where nanoscale zero-valent iron was applied to reduce 2,4,6-trinitrotoluene. However, the  $K_{obs}$  and Fe/Cu dosage does not have a good linear relationship at the second stage (10–40 min), because the major PNP has been degraded at the initial stage. It is also observed from Fig. 6 that the PNP removal efficiency is above 98% after 40 min treatment when the Fe/Cu dosage >35 g/L. Therefore, the optimal Fe/Cu dosage is 35 g/L when the 500 mg/L of PNP aqueous solutions is treated by Fe/Cu bimetallic system. Additionally, the optimal Fe/Cu dosage would be varied with the initial PNP concentration. So it is necessary to optimize the Fe/Cu dosage when the wastewater with a different initial concentration was treated by the Fe/Cu bimetallic system.

### 3.4.3. Effect of initial PNP concentration on the catalytic reactivity

Fig. 7(a) shows the influence of initial PNP concentration on the PNP removal efficiency by the Fe/Cu bimetallic particles, and the  $K_{obs}$  decreases from 0.3352 to 0.0559 min<sup>-1</sup> with the increasing initial PNP concentration from 100 to 1000 mg/L at the initial stage

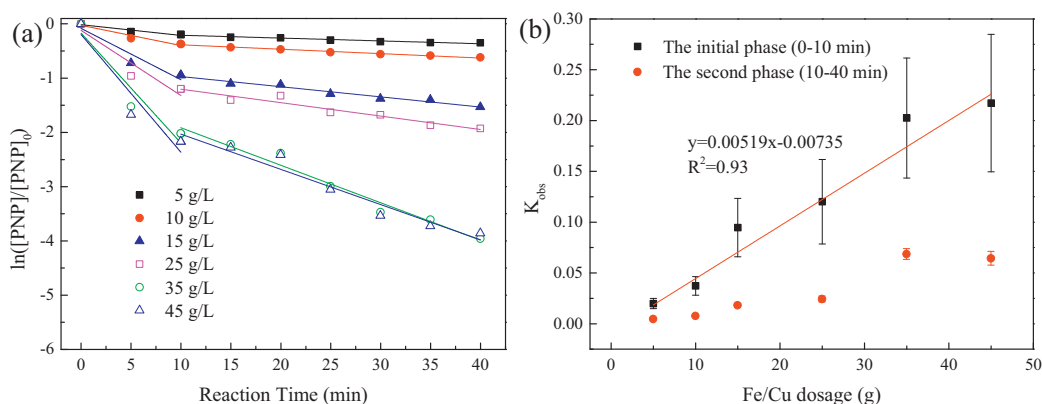


**Fig. 6.** Degradation kinetics for PNP by the prepared Fe/Cu bimetallic particles with different Fe/Cu bimetallic dosage. Experiment conditions were:  $[PNP]_0 = 500$  mg/L, initial pH = 6.7,  $[Na_2SO_4]_0 = 50$  mmol/L, the theoretical Cu mass loading was 0.89 g Cu/g Fe, stirring speed was 400 r/min.

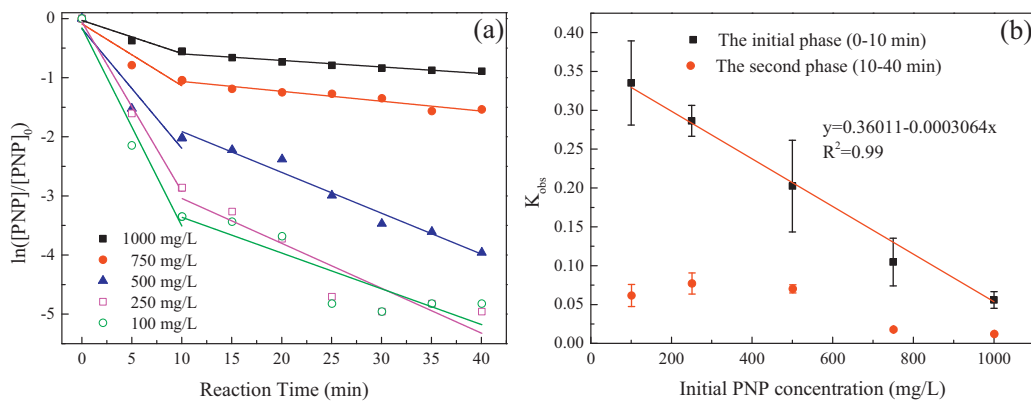


**Fig. 7.** Degradation kinetics for PNP by the prepared Fe/Cu bimetallic particles with different initial PNP concentration. Experiment conditions were: initial pH = 6.7,  $[\text{Na}_2\text{SO}_4]_0 = 50 \text{ mmol/L}$ ,  $[\text{Fe}/\text{Cu}]_0 = 35 \text{ g/L}$ , the theoretical Cu mass loading was 0.89 g Cu/g Fe, stirring speed was 400 r/min.

(0–10 min) (Table S3, Supporting information). Fig. 7(b) shows that the data were plotted as the  $K_{obs}$  against the initial PNP concentration. At the initial stage (0–10 min), the  $K_{obs}$  and PNP concentration have a good linear relationship and the correlation of determination ( $R^2$ ) reaches 0.99, which suggests that the  $K_{obs}$  is proportional to the initial PNP concentration and  $K_{obs}$  can be decreased by elevating the initial PNP concentration. This phenomenon can be explained that more intermediates on the surface of catalysts will occupy catalytic sites or compete with the original pollutants for catalytic sites when the initial PNP concentration increases [33,34]. Furthermore, this problem can only be resolved by improving the mass transport rates of intermediates, products and reactants between the solution phase and the Fe/Cu surface [1,31].

#### 3.4.4. Effect of initial pH on the catalytic reactivity

The effect of initial pH on the PNP removal efficiency by the Fe/Cu bimetallic particles is shown in Fig. 8(a)–(b). Meanwhile, in order to compare the catalytic reactivity of Fe/Cu bimetallic particles with ZVI, ZVI control experiment was setup, and other operating conditions of the control experiment were in accordance with those of the Fe/Cu bimetallic system. Additionally, the effect of initial pH on the PNP degradation by the ZVI system is shown in Fig. 8(c)–(d).

Fig. 8(a) illustrates that the PNP degradation by Fe/Cu bimetallic system with different initial pH all followed the pseudo-first-order kinetics model and the pseudo-first-order kinetic parameters are listed in Table S4 (Supporting information). Fig. 8(b) shows that the data are plotted as the  $K_{obs}$  against the initial pH (3.0–9.0). At the initial stage (0–10 min), the  $K_{obs}$  and initial pH have a good linear relationship and the correlation of determination ( $R^2$ ) reaches 1.00, which suggests that the  $K_{obs}$  is proportional to the initial pH and  $K_{obs}$  can be decreased by elevating the initial pH. According to Fig. 8(c), it is clear that the PNP degradation by ZVI system at different initial pH also followed the pseudo-first-order kinetics model and the pseudo-first-order kinetic parameters are listed in Table S5 (Supporting information). Fig. 8(d) shows that the  $K_{obs}$  of ZVI system and initial pH have a good linear relationship and the correlation of determination ( $R^2$ ) reaches 1.00, only when the initial pH value is lower than 7.0.

By comparing the results of Fe/Cu bimetallic particles and ZVI with different initial pH (3.0–9.0), it can be found that their  $K_{obs}$  decrease with the increasing the initial pH, but the  $K_{obs}$  of Fe/Cu bimetallic particles are always much higher than that of ZVI at the whole pH variation range (3.0–9.0). At the alkaline condition (initial pH 9.0),  $K_{obs}$  of Fe/Cu bimetallic particles ( $0.0643 \text{ min}^{-1}$ ) was 29 times higher than that of ZVI ( $0.0022 \text{ min}^{-1}$ ). Additionally, the PNP removal efficiency of Fe/Cu bimetallic system with initial pH 9.0 still reached approximately 60%, while that of ZVI system was

only approximately 8%. The phenomenon can be explained by the mechanism of Fe/Cu bimetallic particles and ZVI. In ZVI system, the degradation of pollutants is mainly resulted from the  $[\text{H}]_{abs}$  generated by the reaction of Fe and  $\text{H}^+$  (Eqs. (2)–(3)) at the acidic and anaerobic conditions [1,36–39]. In Fe/Cu bimetallic particles system, the degradation of pollutants is mainly resulted from two aspects, (a) direct reduction by accepted electron from the oxidation of Fe at the catalytic activity site (Cu) [13], and a high reaction potential of 0.777 V between Cu and Fe can improve the electron emission rate of Fe [14], (b) indirect reduction by the generated  $[\text{H}]_{abs}$  [21], and the formation mechanism of  $[\text{H}]_{abs}$  in the Fe/Cu system is similar to that in the ZVI system, but the transition metal additives can facilitate the generation of  $[\text{H}]_{abs}$  [20,40]. According to Eqs. (2)–(3), it is clear that  $\text{H}^+$  concentration is a key factor for the formation of  $[\text{H}]_{abs}$ . In other words, the generated rate of  $[\text{H}]_{abs}$  will increase quickly with the increasing  $\text{H}^+$  concentration. Thus the PNP removal efficiencies of ZVI and Fe/Cu increased quickly with the decrease of the initial pH. However, the degradation of PNP by Fe/Cu system was not all resulted from the generated  $[\text{H}]_{abs}$ , and the direct reduction at the catalytic activity site (Cu) also contribute to the PNP degradation. Therefore, approximately 60% PNP removal efficiency was still obtained by the Fe/Cu system even with an initial pH value of 9.0.

Anode (oxidation):



$$E^\theta \left( \frac{\text{Fe}^{2+}}{\text{Fe}} \right) = -0.44 \text{ V}$$

Cathode (reduction, acidic without oxygen):



$$E^\theta \left( \frac{\text{H}^+}{\text{H}_2} \right) = -0.00 \text{ V}$$

#### 3.4.5. Effect of electrolyte ( $\text{Na}_2\text{SO}_4$ ) on the catalytic reactivity

Fig. 9(a) shows the influence of initial  $\text{Na}_2\text{SO}_4$  (as electrolyte) concentration on the PNP removal efficiency by the Fe/Cu bimetallic particles, and the  $K_{obs}$  increases from  $0.0204$  to  $0.2025 \text{ min}^{-1}$  with the increase of the initial PNP concentration from 0 to  $50 \text{ mmol/L}$  at the initial stage (0–10 min) (Table S6, supporting information). Fig. 9(b) shows that the data are plotted as the  $K_{obs}$  against the initial  $\text{Na}_2\text{SO}_4$  concentration, which illustrate that the  $K_{obs}$  and initial  $\text{Na}_2\text{SO}_4$  concentration have a good linear relationship. However, the  $K_{obs}$  at the initial stage ( $[\text{Na}_2\text{SO}_4]_0 < 10 \text{ mmol/L}$ ) is seven times higher than that at the second stage ( $[\text{Na}_2\text{SO}_4]_0 > 10 \text{ mmol/L}$ ). In

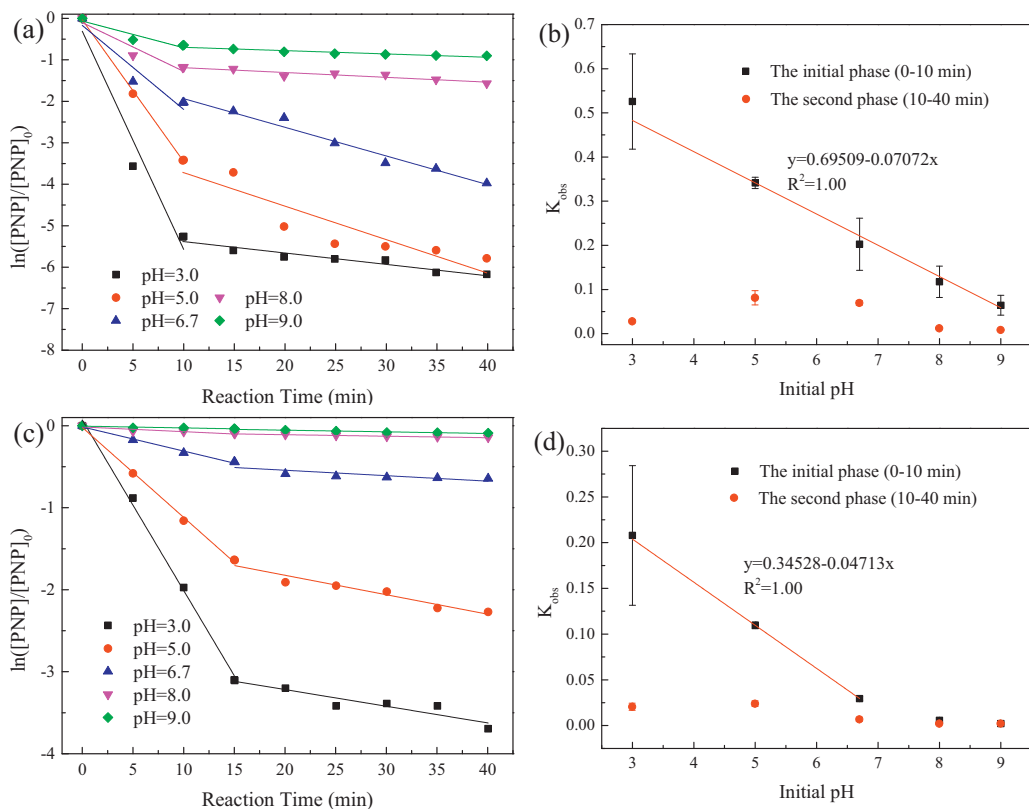


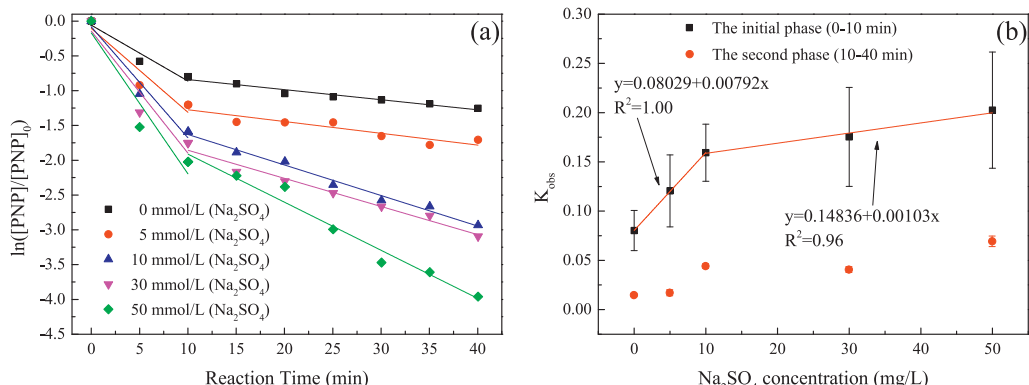
**Fig. 8.** Degradation kinetics for PNP by ((a)–(b)) Fe/Cu bimetallic particles and ((c)–(d)) zero valent iron ( $\text{Fe}^0$ ) with different initial pH value. Experiment conditions were:  $[\text{PNP}]_0 = 500 \text{ mg/L}$ ,  $[\text{Na}_2\text{SO}_4]_0 = 50 \text{ mmol/L}$ ,  $[\text{Fe}/\text{Cu}]_0 = 35 \text{ g/L}$ ,  $[\text{Fe}^0]_0 = 35 \text{ g/L}$ , the theoretical Cu mass loading was  $0.89 \text{ g Cu/g Fe}$ , stirring speed was  $400 \text{ r/min}$ .

other words, the improvement of PNP degradation by  $\text{Na}_2\text{SO}_4$  will not increase obviously when the initial  $\text{Na}_2\text{SO}_4$  concentration is higher than  $10 \text{ mmol/L}$ .  $\text{Na}_2\text{SO}_4$  as an electrolyte can be used to transfer electrons between pollutants and catalytic activity site (Cu), which facilitates the degradation of PNP by Fe/Cu system. Additionally, the previous authors also found that the electrolyte could transfer charge between anodic sites (where Fe oxidation takes place) and cathodic sites (where both  $\text{H}_2\text{O}$  and  $\text{O}_2$  reductions take place), which promoting the pollutant removal efficiency of ZVI system [41].

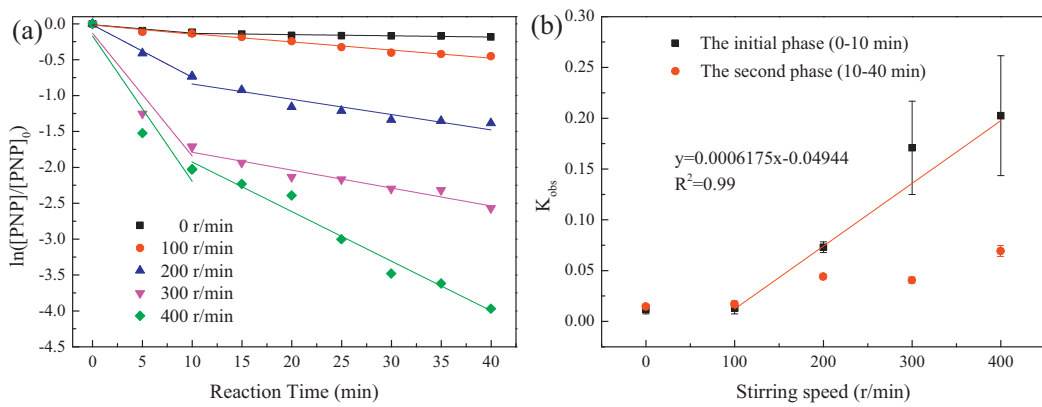
#### 3.4.6. Effect of stirring speed on the catalytic reactivity

Fig. 10(a) shows the influence of stirring speed on the PNP removal efficiency by the Fe/Cu bimetallic particles, and the  $K_{\text{obs}}$  increases from  $0.0118 \text{ min}^{-1}$  to  $0.2025 \text{ min}^{-1}$  with the increase of

stirring speed from 0 to  $400 \text{ r/min}$  at the initial stage (0–10 min) (Table S7, supporting information). Fig. 9(b) shows that the data were plotted as the  $K_{\text{obs}}$  against the stirring speed, which illustrates that the  $K_{\text{obs}}$  and stirring speed have a good linear relationship. The PNP removal efficiency reached approximately 98% at a high stirring speed ( $400 \text{ r/min}$ ), while it was only approximately 18% without mixing. The improvement of PNP degradation was mainly resulted from two aspects, (a) a high stirring speed could enhance the mass transport rates of intermediates, products and reactants between the solution phase and the Fe/Cu surfaces. And the high mass transport rates could promote treatment capacity of the catalysts [1,31]. (b) The high stirring speed facilitated dissolved oxygen (DO) increase in reaction solution. In other words, the oxygen in air is easy to be dissolved into the reaction solution under the condition of high stirring speed. The previous studies have indicated



**Fig. 9.** Degradation kinetics for PNP by the prepared Fe/Cu bimetallic particles with different  $\text{Na}_2\text{SO}_4$  concentration. Experiment conditions were: initial pH = 6.7,  $[\text{PNP}]_0 = 500 \text{ mg/L}$ ,  $[\text{Fe}/\text{Cu}]_0 = 35 \text{ g/L}$ , the theoretical Cu mass loading was  $0.89 \text{ g Cu/g Fe}$ , stirring speed was  $400 \text{ r/min}$ .



**Fig. 10.** Degradation kinetics for PNP by the prepared Fe/Cu bimetallic particles with different stirring speed. Experiment conditions were: initial pH = 6.7,  $[{\text{PNP}}_0] = 500 \text{ mg/L}$ ,  $[\text{Fe}/\text{Cu}]_0 = 35 \text{ g/L}$ ,  $[\text{Na}_2\text{SO}_4]_0 = 50 \text{ mmol/L}$ , the theoretical Cu mass loading was 0.89 g Cu/g Fe, stirring speed was 400 r/min.

that iron corrosion in the presence of oxygen and  $\text{H}^+$  can generate hydrogen peroxide ( $\text{H}_2\text{O}_2$ ), then it can react with the  $\text{Fe}^{2+}$  and produce hydroxyl radical ( $\text{OH}^\bullet$ ) [42,43]. Therefore, not only reduction but also oxidation plays a leading role on the PNP degradation in Fe/Cu system.

### 3.5. COD and TOC removal efficiencies of PNP

The COD and TOC removal efficiencies of the Fe/Cu system and ZVI control experiment are shown in Fig. 11. The curves of Fe/Cu system show that COD and TOC removal efficiencies increased gradually to 21.2% and 22.8% after 40 min treatment, respectively. Meanwhile, the curves of ZVI control experiment show that both COD and TOC removal efficiencies both increased gradually to approximately 8.8%. In the whole 40 min treatment process, the COD and TOC removal efficiencies of Fe/Cu system were much higher than those of ZVI control experiment. The results also reveal that the Cu deposited on the surface of  $\text{Fe}^0$  particles can improve the pollutants degradation capacity of ZVI system obviously. Also, the previous studies suggest that the transition metal (i.e., Cu) can enhance the catalytic reactivity of  $\text{Fe}^0$  [20–22]. And Cu can enhance the corrosion rate of Fe due to the high reaction potential (0.777 V) between Cu and Fe [14]. In other word, Cu can facilitate the

generation of surface-bond atomic hydrogen ( $[\text{H}]_{\text{abs}}$ ), which could improve the reduction capacity of Fe [20,21]. Therefore, the Cu deposited on the surface of  $\text{Fe}^0$  particles can improve the pollutants degradation capacity of ZVI system obviously.

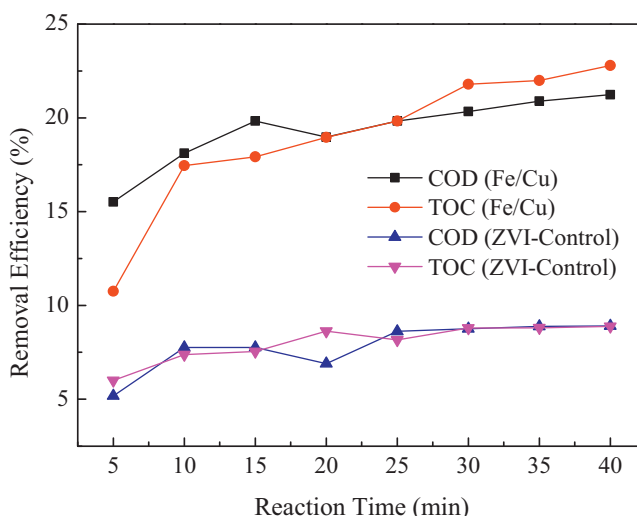
### 3.6. UV-vis and FTIR spectral analysis

The UV-vis spectra of the influent and effluent of ZVI and Fe/Cu system with different treatment time (0–40 min) are shown in Fig. 12. In our previous work, it is clear that the peak at 227 nm is mainly attributed to the  $\pi-\pi^*$  transition of benzene ring of monoaromatics [11], and the peak at 317 nm is mainly due to the conjugation of benzene ring and chromophoric group (i.e.,  $-\text{NO}_2$ ).

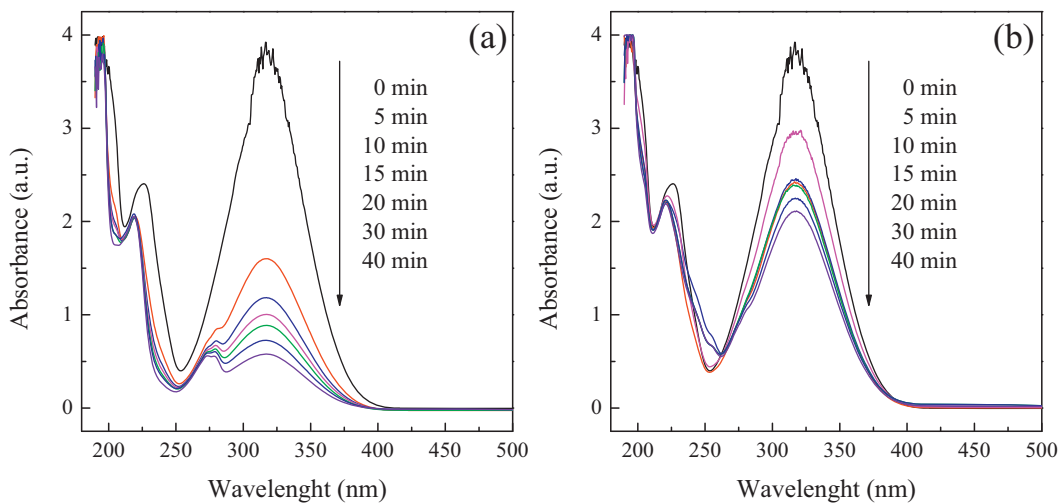
Fig. 12(a) shows the variation of ultraviolet adsorption spectra of the influent and effluent of Fe/Cu bimetallic system under different treatment time. It is observed that absorbance intensity of the peak at 317 nm decreased strongly in the 40 min treatment process, while that of the peak at 227 nm dropped a little. The results suggest that the  $-\text{NO}_2$  on the molecular structure of PNP be reduced effectively by the Fe/Cu bimetallic system, while only a little part of benzene ring of PNP be opened and mineralized. The results of UV-vis spectra are in accordance with the obtained lower TOC and COD removal efficiencies (approximately 20%). Fig. 12(b) shows the variation of ultraviolet adsorption spectra of the influent and effluent of ZVI control experiment. It is observed that the absorbance intensity of the peak at 317 nm dropped slowly in the treatment process, and that of the peak at 227 nm has scarcely changed in this process. The results reveal that only a little part of PNP can be removed by the ZVI system. Therefore, the catalytic capacity of the prepared Fe/Cu bimetallic particles is much stronger than that of the traditional ZVI.

Fig. 13 shows the FTIR adsorption spectra of the influent and effluent of the ZVI and Fe/Cu system under the same conditions. The absorbance bands are interpreted by information from prior reports [11,44–46].

Fig. 13(a) is the FTIR adsorption spectrum of the influent (PNP) of the Fe/Cu and ZVI system. The band at  $3324 \text{ cm}^{-1}$  is attributed to the stretching vibration of O-H and hydrogen-bonded O-H [44]; the bands at  $3120$  and  $3080 \text{ cm}^{-1}$  are attributed to the stretching vibration of aromatic C-H [44]; the bands at  $1495$ ,  $1515$ ,  $1590$  and  $1613 \text{ cm}^{-1}$  are attributed to the overlap of the aromatic C=C skeletal vibration and the aromatic  $-\text{NO}_2$  asymmetrical stretching vibration [47]; the band at  $1326 \text{ cm}^{-1}$  is attributed to the symmetrical stretching vibration of aromatic  $-\text{NO}_2$  [48,49]; the bands at  $1109$ ,  $1164$ ,  $1216$  and  $1283 \text{ cm}^{-1}$  are attributed to in-plane bending vibration of =C-H on the benzene ring [48]; the band at  $851 \text{ cm}^{-1}$  is attributed to out-of-plane bending vibration of =C-H on the



**Fig. 11.** The COD and TOC removal efficiencies of PNP (500 mg/L) aqueous solution by using Fe/Cu bimetallic particles or ZVI. Experiment conditions were: initial pH = 6.7,  $[{\text{PNP}}_0] = 500 \text{ mg/L}$ , COD<sub>0</sub> = 866 mg/L, TOC<sub>0</sub> = 252 mg/L,  $[\text{Na}_2\text{SO}_4]_0 = 50 \text{ mmol/L}$ ,  $[\text{Fe}/\text{Cu}]_0 = 35 \text{ g/L}$ ,  $[\text{Fe}^0]_0 = 35 \text{ g/L}$ , the theoretical Cu mass loading was 0.89 g Cu/g Fe, stirring speed was 400 r/min.



**Fig. 12.** The variation of UV-vis spectra of PNP (500 mg/L) aqueous solution during the treatment process by using Fe/Cu bimetallic particles or ZVI. Experiment conditions were: initial pH = 6.7,  $[PNP]_0 = 500 \text{ mg/L}$ ,  $[Na_2SO_4]_0 = 50 \text{ mmol/L}$ ,  $[Fe/Cu]_0 = 35 \text{ g/L}$ ,  $[Fe^0]_0 = 35 \text{ g/L}$ , the theoretical Cu mass loading was 0.89 g Cu/g Fe, stirring speed was 400 r/min.

benzene ring with the para-orienting groups (i.e.,  $-NO_2$  and  $-OH$ ) [50]. The results of FTIR adsorption spectrum show that the main pollutant in the influent is PNP.

**Fig. 13(b)** is the FTIR adsorption spectrum of the effluent of the ZVI control experiment after 60 min treatment. This spectrum shows that all the transmission (%) of the main bands at 1326, 1495, 1515, 1590 and  $1613 \text{ cm}^{-1}$  increased, but they did not removed completely after 60 min treatment by ZVI system. The results reveal that only a part of PNP in aqueous solution can be degraded by the ZVI system (60 min). Additionally, the bands at 1109, 1164, 1216 and  $1283 \text{ cm}^{-1}$  were changed into a broad band at  $1119 \text{ cm}^{-1}$ , which might be resulted from the formation of hydrogen-bonded O-H between the degradation products (such as the compounds with  $-C-H$ ,  $-O-H$ ,  $-C-O$  or  $-N-H$ ).

**Fig. 13(c)** is the FTIR adsorption spectrum of the effluent of the Fe/Cu experiment after 40 min treatment. This spectrum shows that the main bands at 1326, 1495, 1515, 1590 and  $1613 \text{ cm}^{-1}$  almost removed completely after 40 min treatment by ZVI system. The results reveal that most of  $-NO_2$  on PNP has been removed by the Fe/Cu system, which are consistent with the PNP removal efficiency (approximately 98%) after 40 min treatment. Additionally, the bands at 1109, 1164, 1216 and  $1283 \text{ cm}^{-1}$  were changed into a broad band at  $1139 \text{ cm}^{-1}$ , which might be resulted from the formation of hydrogen-bonded O-H between the degradation products

(such as the compounds with  $-C-H$ ,  $-O-H$ ,  $-C-O$  or  $-N-H$ ). By the comparison between the FTIR spectra of **Fig. 13(a)** and (b), it can be concluded that the pollutant degradation capacity of Fe/Cu is much stronger than that of ZVI.

### 3.7. Iron and copper leaching during the process

The pollutant degradation capacity of Fe/Cu bimetallic system or ZVI was usually correlated with the corrosion of  $Fe^0$  [30,41,51]. In the Fe/Cu bimetallic system,  $Cu^0$  was a catalyst to facilitate the corrosion of  $Fe^0$  [21,30]. Therefore, the  $Cu^0$  could not leach during the process, and no  $Cu^{2+}$  was detected in the effluent. During the treatment process, the main corrosion products of  $Fe^0$  would be discharged with the formation of  $Fe^{2+}$ ,  $Fe^{3+}$ ,  $Fe(OH)_2$  or  $Fe(OH)_3$ . After 40 min treatment, the total Fe concentration (34.1 mg/L) in the effluent of Fe/Cu bimetallic system was higher than that (26.2 mg/L) of ZVI control experiment. The results suggest that the corrosion of  $Fe^0$  could be improved by  $Cu^0$ , which resulting in the higher catalytic reactivity of Fe/Cu bimetallic particles.

### 3.8. Proposed reaction pathway for the destruction of PNP

The intermediates in the degradation of PNP by the Fe/Cu bimetallic system were identified by GC/MS analysis. The

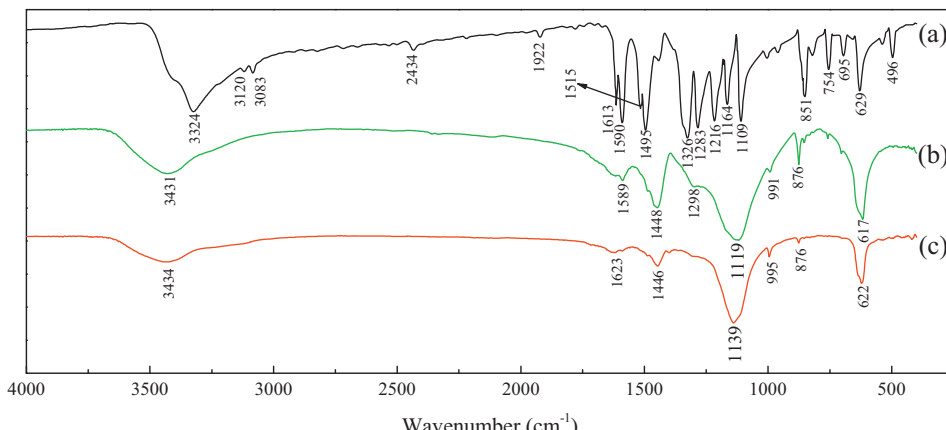


**Fig. 13.** The FTIR adsorption spectra of 400–4000  $\text{cm}^{-1}$  region of influent and effluent: (a) influent, (b) effluent of ZVI (60 min), (c) effluent of Fe/Cu (40 min). Experiment conditions were: initial pH = 6.7,  $[PNP]_0 = 500 \text{ mg/L}$ ,  $[Na_2SO_4]_0 = 50 \text{ mmol/L}$ ,  $[Fe/Cu]_0 = 35 \text{ g/L}$ ,  $[Fe^0]_0 = 35 \text{ g/L}$ , the theoretical Cu mass loading was 0.89 g Cu/g Fe, stirring speed was 400 r/min.

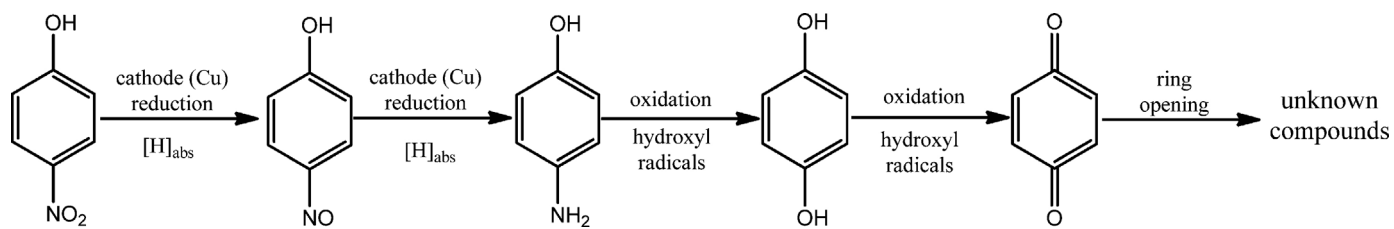


**Fig. 14.** Proposed reaction pathway for the degradation of PNP by using Fe/Cu bimetallic particles. Experiment conditions were: initial pH = 6.7,  $[PNP]_0 = 500 \text{ mg/L}$ ,  $[\text{Na}_2\text{SO}_4]_0 = 50 \text{ mmol/L}$ ,  $[\text{Fe}/\text{Cu}]_0 = 35 \text{ g/L}$ , the theoretical Cu mass loading was 0.89 g Cu/g Fe, stirring speed was 400 r/min.

intermediates detected include *p*-aminophenol (18.95 min), hydroquinone (18.88 min), *p*-benzoquinone (13.11 min) and three unknown compounds (Figs. S1 and S2, supporting information). The 4-nitrosophenol is not detected by GC/MS analysis. It can be explained that 4-nitrosophenol might be reduced into *p*-aminophenol instantaneously when it is produced in the degradation process. Thus the 4-nitrosophenol is hard to be detected in the treatment effluent. However, the 4-nitrosophenol should be presented in the degradation pathway based on the previous studies [52]. The main degradation pathway is proposed in Fig. 14. PNP is first reduced to 4-nitrosophenol by direct reduction on catalytic activity site (Cu) or indirect reduction of  $[\text{H}]_{\text{abs}}$ , which is further reduced to *p*-aminophenol. Then *p*-aminophenol is oxidized to hydroquinone and *p*-benzoquinone by hydroxyl radicals. Finally, the benzene ring of *p*-benzoquinone can be opened by hydroxyl radicals and further oxidized to ring opening compounds (such as small molecule organic acid). According to the previous studies, it is clear that these products exhibited the lower toxicity and higher biodegradability than their parent compound (i.e., PNP) [53–58]. The degradation pathway of PNP by Fe/Cu bimetallic system is similar to that by cathode reduction and electro-Fenton methods [52]. However the PNP cannot be mineralized completely by Fe/Cu bimetallic system. What's more, only approximately 20% COD and TOC removal efficiency was obtained after 40 min treatment by the Fe/Cu bimetallic system, which also proved that only a little part of PNP could be mineralized. In addition, there was no ring opening compound was detected by GC/MS analysis. The results reveal that the ring opening reaction of the *p*-benzoquinone almost did not occur in the treatment process. The phenomenon can be explained that the amount of the generated hydroxyl radicals was not enough for the ring opening reaction due to the high initial PNP concentration (500 mg/L). Although the Fe/Cu bimetallic system cannot mineralize the PNP completely, it can transfer PNP in aqueous solution into the nontoxic and biodegradable intermediate products. Therefore, the Fe/Cu bimetallic system can be proposed as a cost-effective pretreatment process for the toxic and refractory PNP wastewater. And this technology also could extend to improve the biodegradability of the complicated, toxic and refractory industrial wastewater.

#### 4. Conclusions

The prepared Fe/Cu bimetallic particles with different theoretical copper mass loadings (0.05, 0.11, 0.24, 0.41, 0.62, 0.89, 1.26 and 1.81 g Cu/g Fe) were characterized by SEM, EDS, XRD and laser particle size analyzer. It was observed that a large number of fine Cu particles ( $1\text{--}40 \mu\text{m}$ ) were produced from the excessive theoretical Cu mass loading, and they can facilitate the catalytic reactivity of the Fe/Cu bimetallic particles at Cu loading  $<0.89 \text{ g Cu/g Fe}$ . The heterogeneous Cu layer on surface of Fe/Cu bimetallic particle can facilitate its pollutant degradation, while the uniform and dense Cu layer will decrease its reactivity seriously. Furthermore, the optimal operating parameters (initial pH = 6.7,  $[\text{Na}_2\text{SO}_4]_0 = 50 \text{ mmol/L}$ ,  $[\text{Fe}/\text{Cu}]_0 = 35 \text{ g/L}$ , the theoretical

copper mass loadings of 0.89 g Cu/g Fe, stirring speed of 400 r/min) were obtained by batch experiments. Under the optimal conditions, the PNP, COD and TOC removal efficiencies reached approximately 98.0%, 21.2% and 22.8%, respectively, after 40 min treatment by the Fe/Cu bimetallic system, whereas those of ZVI control experiments only reached approximately 47.2%, 8.9% and 8.9%, respectively. The results indicate that the pollutant degradation capacity of the Fe/Cu bimetallic system was much higher than that of the traditional ZVI system. Additionally, the detected results of UV-vis and FTIR spectra also proved that the catalytic reactivity of Fe/Cu bimetallic particles was much stronger than that of ZVI. The degradation rates of PNP by the Fe/Cu particles with different theoretical Cu mass loadings are all in accordance with the pseudo-first-order kinetics model, and the degradation of PNP was resulted from the synergistic reaction of indirect reduction by atomic hydrogen and direct reduction on the catalytic activity sites. According to the detected intermediates by GC/MS, it can be concluded that the Fe/Cu bimetallic system can transfer PNP into the nontoxic and biodegradable intermediate products. Therefore, these results suggest that the Fe/Cu bimetallic system can extend to improve the biodegradability of the complicated, toxic and refractory industrial wastewater.

#### Acknowledgment

The authors would like to acknowledge the financial support from national natural science foundation of China (No. 21207094), China postdoctoral science foundation special funded project (No. 2013T60854) and special S&T project on treatment and control of water pollution (No. 2012ZX07201-005).

#### Appendix A. Supplementary data

Supplementary data associated with this article can be found, in the online version, at <http://dx.doi.org/10.1016/j.apcatb.2013.08.020>.

#### References

- [1] B. Lai, Z.Y. Chen, Y.X. Zhou, P. Yang, J.L. Wang, Z.Q. Chen, Journal of Hazardous Materials 250–251 (2013) 220–228.
- [2] Z.I. Bhatti, H. Toda, K. Furukawa, Water Research 36 (2002) 1135–1142.
- [3] S.Q. Yu, J. Hu, J.L. Wang, Journal of Hazardous Materials 177 (2010) 1061–1067.
- [4] M. Pimentel, N. Oturan, M. Dezotti, M.A. Oturan, Applied Catalysis B: Environmental 83 (2008) 140–149.
- [5] G. Mele, G. Ciccarella, G. Vasapollo, E. Garcíá-López, L. Palmisano, M. Schiavello, Applied Catalysis B: Environmental 38 (2002) 309–319.
- [6] C. Wang, J. Li, G. Mele, G.M. Yang, F.X. Zhang, L. Palmisano, G. Vasapollo, Applied Catalysis B: Environmental 76 (2007) 218–226.
- [7] M. Martín-Hernández, J. Carrera, M.E. Suárez-Ojeda, M. Besson, C. Descorme, Applied Catalysis B: Environmental 123–124 (2012) 141–150.
- [8] L.L. Bo, X. Quan, S. Chen, H.M. Zhao, Y.Z. Zhao, Water Research 40 (2006) 3061–3068.
- [9] S.H. Chang, K.S. Wang, S.J. Chao, T.H. Peng, L.C. Huang, Journal of Hazardous Materials 166 (2009) 1127–1133.
- [10] G. Kim, W. Jeong, S. Choe, Journal of Hazardous Materials 155 (2008) 502–506.
- [11] B. Lai, Y.X. Zhou, H.K. Qin, C.Y. Wu, C.C. Pang, Y. Lian, J.X. Xu, Chemical Engineering Journal 179 (2012) 1–7.

- [12] B. Lai, Y.X. Zhou, P. Yang, *Industrial and Engineering Chemistry Research* 51 (2012) 7777–7785.
- [13] W.Y. Xu, T.Y. Gao, *Journal of Environmental Sciences* 19 (2007) 792–799.
- [14] L.M. Ma, Z.G. Ding, T.Y. Gao, R.F. Zhou, W.Y. Xu, J. Liu, *Chemosphere* 55 (2004) 1207–1212.
- [15] J.H. Fan, L.M. Ma, *Journal of Hazardous Materials* 164 (2009) 1392–1397.
- [16] J.P. Fennelly, A.L. Roberts, *Environmental Science and Technology* 32 (1998) 1980–1988.
- [17] Y.H. Kim, E.R. Carraway, *Environmental Science and Technology* 34 (2000) 2014–2017.
- [18] A. Koutsospyros, J. Pavlov, J. Fawcett, D. Strickland, B. Smolinski, W. Braida, *Journal of Hazardous Materials* 219–220 (2012) 75–81.
- [19] C.H. Wan, Y.H. Chen, R. Wei, *Environmental Toxicology and Chemistry* 18 (1999) 1091–1096.
- [20] C.J. Lin, S.L. Lo, Y.H. Liou, *Journal of Hazardous Materials* 116 (2004) 219–228.
- [21] S.J. Bransfield, D.M. Cwiertny, K. Livi, D.H. Fairbrother, *Applied Catalysis B: Environmental* 76 (2007) 348–356.
- [22] D.M. Cwiertny, S.J. Bransfield, K.J.T. Livi, D.H. Fairbrother, A.L. Roberts, *Environmental Science and Technology* 40 (2006) 6837–6843.
- [23] H.L. Lien, W.X. Zhang, *Chemosphere* 49 (2002) 371–378.
- [24] S.J. Bransfield, D.M. Cwiertny, A.L. Roberts, D.H. Fairbrother, *Environmental Science and Technology* 40 (2006) 1485–1490.
- [25] B. Lai, Y.X. Zhou, P. Yang, *Chemical Engineering Journal* 200–202 (2012) 10–17.
- [26] C. Grittini, M. Malcomson, Q. Fernando, N. Korte, *Environmental Science and Technology* 29 (1995) 2898–2900.
- [27] F. Braun, A.M. Tarditi, L.M. Cornaglia, *Journal of Membrane Science* 382 (2011) 252–261.
- [28] F. Hanna, Z.A. Hamid, A.A. Aal, *Materials Letters* 58 (2004) 104–109.
- [29] F. Qi, B.B. Xu, L. Zhao, Z.L. Chen, L.Q. Zhang, D.Z. Sun, J. Ma, *Applied Catalysis B: Environmental* 121–122 (2012) 171–181.
- [30] D.M. Cwiertny, S.J. Bransfield, A.L. Roberts, *Environmental Science and Technology* 41 (2007) 3734–3740.
- [31] H.M. Hung, F.H. Ling, M.R. Hoffmann, *Environmental Science and Technology* 34 (2000) 1758–1763.
- [32] B. Lai, Y.X. Zhou, P. Yang, J.H. Yang, J.L. Wang, *Chemosphere* 90 (2013) 1470–1477.
- [33] H.Y. Shu, M.C. Chang, C.C. Chen, P.E. Chen, *Journal of Hazardous Materials* 184 (2010) 499–505.
- [34] X.H. Qiu, Z.Q. Fang, B. Liang, F.L. Gu, Z.C. Xu, *Journal of Hazardous Materials* 193 (2011) 70–81.
- [35] X. Zhang, Y.M. Lin, Z.L. Chen, *Journal of Hazardous Materials* 165 (2009) 923–927.
- [36] Y.L. Jiao, C.C. Qiu, L.H. Huang, K.X. Wu, H.Y. Ma, S.H. Chen, L.M. Ma, D.L. Wu, *Applied Catalysis B: Environmental* 91 (2009) 434–440.
- [37] Y.H. Shih, C.Y. Hsu, Y.F. Su, *Separation and Purification Technology* 76 (2011) 268–274.
- [38] X.T. Liu, W. Zhao, K. Sun, G.X. Zhang, Y. Zhao, *Chemosphere* 82 (2011) 773–777.
- [39] F.K. Kawahara, P.M. Michalakos, *Industrial and Engineering Chemistry Research* 36 (1997) 1580–1585.
- [40] B. Schrick, J.L. Blough, A.D. Jones, T.E. Mallouk, *Chemistry of Materials* 14 (2002) 5140–5147.
- [41] J.M. Triszcza, A. Porta, F.S.G. Einschlag, *Chemical Engineering Journal* 150 (2009) 431–439.
- [42] S.H. Joo, A.J. Feitz, D.L. Sedlak, T.D. Waite, *Environmental Science and Technology* 39 (2004) 1263–1268.
- [43] K.S. Wang, C.L. Lin, M.C. Wei, H.H. Liang, H.C. Li, C.H. Chang, Y.T. Fang, S.H. Chang, *Journal of Hazardous Materials* 182 (2010) 886–895.
- [44] Z. Droussi, V. D'orazio, M.R. Provenzano, M. Hafidi, A. Ouattmane, *Journal of Hazardous Materials* 164 (2009) 1281–1285.
- [45] H.E. Hajjouji, F. Barje, E. Pinelli, J.R. Bailly, C. Richard, P. Winterton, J.C. Revel, M. Hafidi, *Bioresource Technology* 99 (2008) 7264–7269.
- [46] H.E. Hajjouji, N. Fakhredine, G. Ait Baddi, P. Winterton, J.R. Bailly, J.C. Revel, M. Hafidi, *Bioresource Technology* 98 (2007) 3513–3520.
- [47] N. Sundaraganesan, B. Anand, B. Dominic Joshua, *Spectrochimica Acta Part A: Molecular and Biomolecular Spectroscopy* 65 (2006) 1053–1062.
- [48] M. Arivazhagan, S. Jeyavijayan, *Spectrochimica Acta Part A: Molecular and Biomolecular Spectroscopy* 79 (2011) 376–383.
- [49] N. Sundaraganesan, S. Ayyappan, H. Umamaheswari, B. Dominic Joshua, *Spectrochimica Acta Part A: Molecular and Biomolecular Spectroscopy* 66 (2007) 17–27.
- [50] V. Krishnakumar, D. Barathi, R. Mathammal, *Spectrochimica Acta Part A: Molecular and Biomolecular Spectroscopy* 86 (2012) 196–204.
- [51] I.H. Yoon, K.W. Kim, S. Bang, M.G. Kim, *Applied Catalysis B: Environmental* 104 (2011) 185–192.
- [52] S.H. Yuan, M. Tian, Y.P. Cui, L. Lin, X.H. Lu, *Journal of Hazardous Materials* 137 (2006) 573–580.
- [53] X. Hu, A. Li, J. Fan, C. Deng, Q. Zhang, *Bioresource Technology* 99 (2008) 4529–4533.
- [54] B.A. Donlon, E. Razo-Flores, J.A. Field, G. Lettinga, *Applied and Environmental Microbiology* 61 (1995) 3889–3893.
- [55] Ö.S. Kuşçu, D.T. Sponza, *Enzyme and Microbial Technology* 36 (2005) 888–895.
- [56] P. Jiang, J. Zhou, A. Zhang, Y. Zhong, *Journal of Environmental Sciences* 22 (2010) 500–506.
- [57] S. Yuan, M. Tian, Y. Cui, L. Lin, X. Lu, *Journal of Hazardous Materials* 137 (2006) 573–580.
- [58] S. Meriç, H. Selçuk, V. Belgiorne, *Water Research* 39 (2005) 1147–1153.